POAC'19
Delft, The Netherlands

Proceedings of the 25th International Conference on
Port and Ocean Engineering under Arctic Conditions
June 09-13, 2019, Delft, The Netherlands

Analysis of Stamukhi Distribution in the Caspian Sea

Anton Sigitov[1], Yevgeniy Kadranov[1], Sergey Vernyayev[1],

[1] LLP ICEMAN.KZ, Shymkent, Kazakhstan

ABSTRACT

After Kashagan project going into production Industry continues exploring and developing oil fields in the northern part of the Caspian Sea. Pearls, Kalamkas, Kurmangazy, Zhanbay fields are either going through FEED stage or in discussion to launch exploratory drilling. Regardless of their location in the region pipeline is the most feasible way to transport hydrocarbons when in production considering logistical challenges associated with marine transport through shallowing sea. Loading factors from stamukhi (vast grounded ice rubble accumulations) are one of the most significant design criteria for future construction of pipelines. This study illustrates distribution of these features across the region and attempts to analyze dependencies of their appearance from such factors as water depth and proximity to coastline, FDD severity index and wind regime during the winter.

KEY WORDS: FEED; Stamukhi; Remote Sensing; Regional ice monitoring, Operations in ice.

GENERAL

Stamukha is a famous grounded ice rubble feature often observed in mild sub-Arctic conditions of the Caspian Sea. It is normally formed when deeper part of a ridges keel hits seabed and loses speed relative to surrounding drifting ice cover with following rapid growth of rubble piling up together and grounding in one spot. Continuing and recurring drift events only make the pile of rubble bigger both in width and height. While an average stamukha can reach 200-300m in width there are cases when they were observed to reach 1000 m and becoming more a vast anchored to seabed grounded rubble field. Stamukha's height is limited with thickness of drifting ice forming it and was estimated to reach maximum of 16 m by McKenna et all 2011. Typical stamukhi and their look on Sentinel-1 image are shown on Figure 1.

There are several major areas, where knowledge of stamukhi phenomena is important:

1. Pipeline design from offshore structures to shore is based on burial depth depending on frequency and size of stamukhi over areas of planned construction.
2. Marine operations during transition between ice and open water seasons when ice cover is already gone and light hull speed boats with no ice class thriving to go into operations. Stamukhi that still persist are posing a hazard of an unmarked obstacle.
3. Air Cushion Vehicle (ACV) operations through the season are also affected with

stamukhi being a navigational hazard for vessels moving at generally higher speeds than conventional Ice Breaking Supply Vessels (IBSV). Stamukhi also increase general roughness of ice cover surface in the surrounding while promoting ridge formation in addition to other factors.

4. Ice charting operations in support of marine operations rely on spatial distribution of stamukhi data that facilitates ice drift forecast by indicating areas with higher anchoring index affecting drift speed. Accurate drift forecast is vital for ice hazards management both at offshore installations and along confined channels as discussed by Bukharitsyn et all 2019.

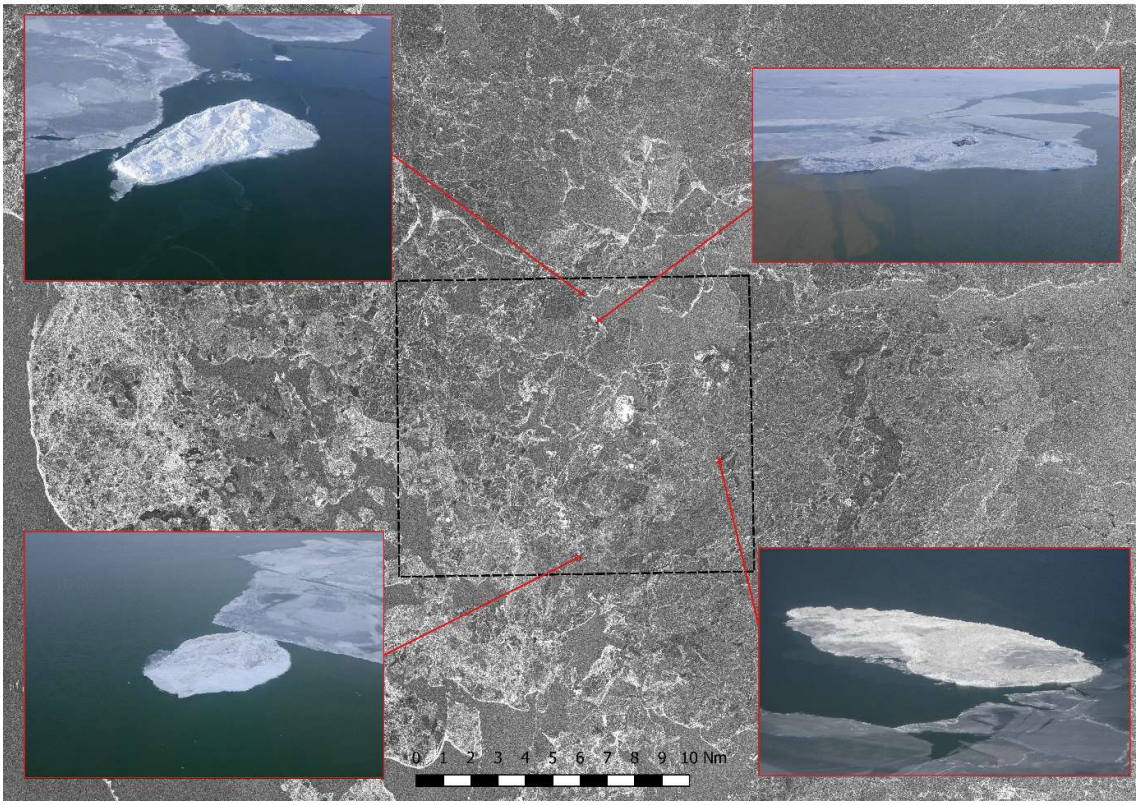

Figure 1: Aerial photos of stamukhi observed during overflight in the vicinity of Kashagan structures and their location as detected with Sentinel-1 SAR image (Vernyayev, et al., 2016).

The last complex study of stamukhi distribution on regional scale and attempt to classify it by Freezing Degree Days (FDD) severity index was published by Hydrometeoizdat, 1992. There were several years of field surveys performed by Agip KCO (Nilsen et al, 2011) on local scale in vicinity of Kashagan in 2000s. And this is almost complete list of studies performed on the matter in the region. ICEMAN.KZ that puts significant emphasis on development of ice charting tools and forecasting techniques has identified significant lack of up-to-date and complete data as well as phenomena knowledge in the area and performed this stamukhi distribution study. With the data collection program and database specifically designed to address both offshore design and operational concerns the study was targeted to:

- update information on distribution of these features across the whole region and develop comprehensive way of presenting and managing data for operational use;
- analyze dependencies of their appearance from such factors as water depth and

proximity to coastline, FDD severity index and wind regime during the winter;
- identify additional categories of data needed to enhance detection techniques and improve or develop forecasting and monitoring services.

The next sections describe our data collection program and structure of database addressing major uncertainties in interpretation of remote sensing data. Further on, we show major dependencies that were identified out of this study and what questions arise from the results.

STAMUKHI DATA COLLECTION PROGRAM AND DATABASE DESCRIPTION

ICEMAN.KZ approach to study stamukhi phenomena in the Caspian Sea has evolved from commercial ice charting program enhanced with internal routines and structured interdisciplinary database purposed to advance ice forecasting techniques in the region. Internal Stamukhi detection program includes the following activities.

Both historical and newly acquired Synthetic Aperture Radar (SAR) images (mainly Sentinel-1 due to unrestricted availability, sufficient resolution, spatial and temporal coverage) and usable Sentinel-2 and Landsat high resolution optical images over the Caspian region are downloaded and refined for ice charting purposes. Database with list of all usable images and their spatial coverage is compiled to evaluate satellite imagery revisit time. This parameter indicates accuracy of detection and erosion dates and, thus, duration of stamukhi persistence.

During an ongoing season once newly acquired image is available on our servers for ice charting analysis, operator on duty performs stamukhi search utilizing internal data management system with the following algorithm:

1) After mobile and stable areas are delineated visual investigation is carried out to spot features containing a point of high response with clear signs of features indicating presence of an obstacle in moving ice (open water channel left in the drifting ice as shown in Figure 2, for example). A lot of targets are found during break-up when opening waters contrast out bright points often with tails of rubble floating downwind. Width of such features is then measured and accordingly recorded.
2) The record also contains attributes of detection and erosion dates. Detection date is confirmed for each feature by backtracking the stack of season's images to confirm the nearest in time image, when a high response feature is traceable and ice conditions indicate possibility of stamukhi formation with corresponding ice drift events. In some cases, features are only found closer to the end of the season are then tracked back to the early days of winter before the area stabilized for the rest of the season.
3) Sentinel-2 and Landsat high resolution cloudless and partly cloudy images through the length of the season are thoroughly investigated to ensure all the uncertainties with interpretation of SAR images over mainly stationary through majority of the season areas of ice cover is removed from the database.

Figure 2: Channels of open water left by stamukhi in drifting ice viewed with Sentinel-2 image acquired on February 20th.

This approach to identifying stamukhi presence, however, has a certain list of uncertainties arising from limits posed by remote sensing in general and control measures that reduce them to increase reliability of the dataset:

- Complexity of individual feature recognition from different satellite platforms is illustrated in Figure 3 and was discussed in detail by Vernyayev et al 2016. The major point here is that various resolution as well as differing sensor types and acquisition modes of both optical and SAR images show stamukhi differently leaving a lot of room for misinterpretation and human error. However, within the scope of this monitoring program this issue is handled with emphasis on consequences of drift events adding reliability to observations collected into the dataset.
- Temporal distribution parameters of stamukhi directly depends on revisit time by satellites and poses the major inaccuracy factor in the early years of observations. Figure 4 illustrates distribution of days between meaningful images during the seasons when detection program was carried out. It should be noted that amount of 5-10 days gaps in revisit time during the first two seasons in the database is significantly higher than in the last three seasons. This is associated with increasing frequency of acquisitions by Sentinel-1A forming the base of the study. Launch of Sentinel-1B and Sentinel-2B has also improved reliability of observations with increasing amount of remote sensing data for analysis.

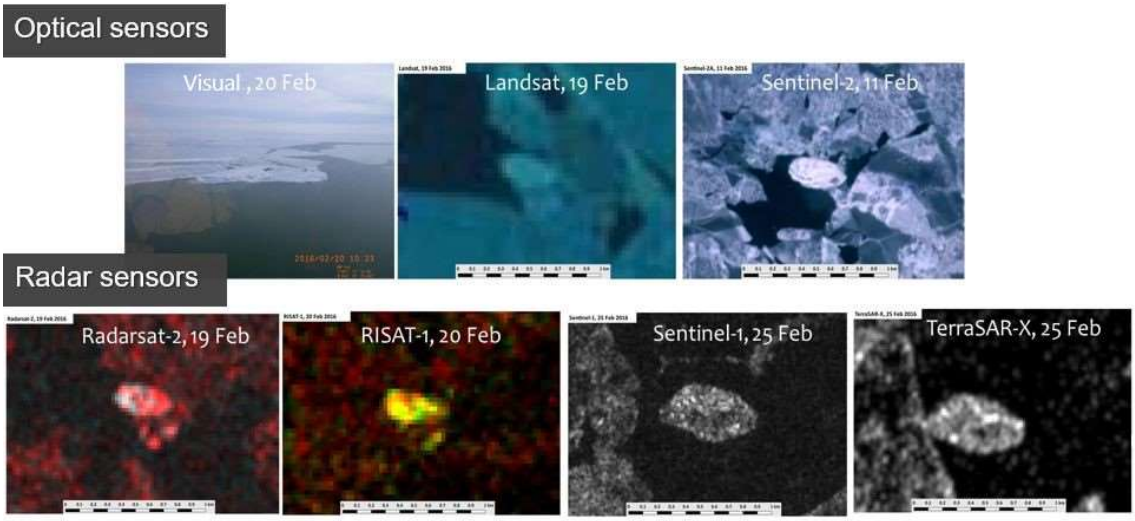

Figure 3: Stamukhi as observed with means of variety of sources: Aerial survey, Optical and SAR satellite images (Vernyayev, et al., 2016).

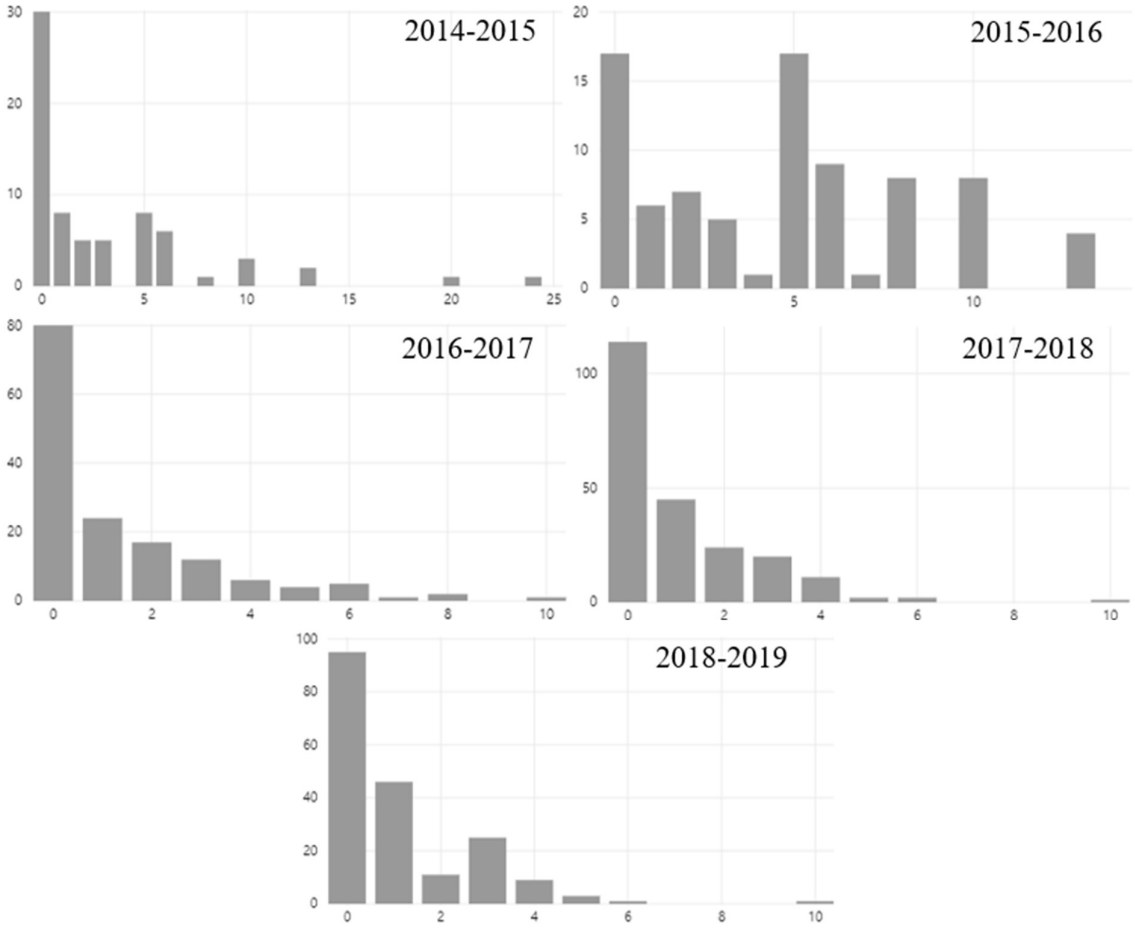

Figure 4: Number of temporal gaps between usable images sorted by duration in days during seasons from 2014 to 2019 (ICEMAN.KZ, 2019).

Once each individual season was processed in such way by one operator and cross-checked by another to reduce bias from human perception all observations were merged into single database. Table 1 summarizes number of usable (cloudless or partly cloudy optical and SAR) images per each season and their amount divided by season length to give unobscured understanding of overall imagery availability per each season. The same table shows number of stamukhi that were identified and recorded by season out of total 3407 records in the database.

Table 1: Summary of input usable images and resulting stamukhi observations in database.

Season	Number of images	Number of images per day	Number of observations
2014-2015	48	0.33	653
2015-2016	49	0.61	420
2016-2017	120	0.91	353
2017-2018	153	1.23	932
2018-2019	157	1.19	1049

Figure 5 illustrates distribution of all stamukhi observations for winter seasons during the last 5 years over the whole region and forming the source database for further analysis. Bathymetry layer in the background was used at later stages to define water depth at the site of each individual stamukha based on annual average sea level changing through the seasons and neglecting wind induced water level fluctuations in the scope of this study.

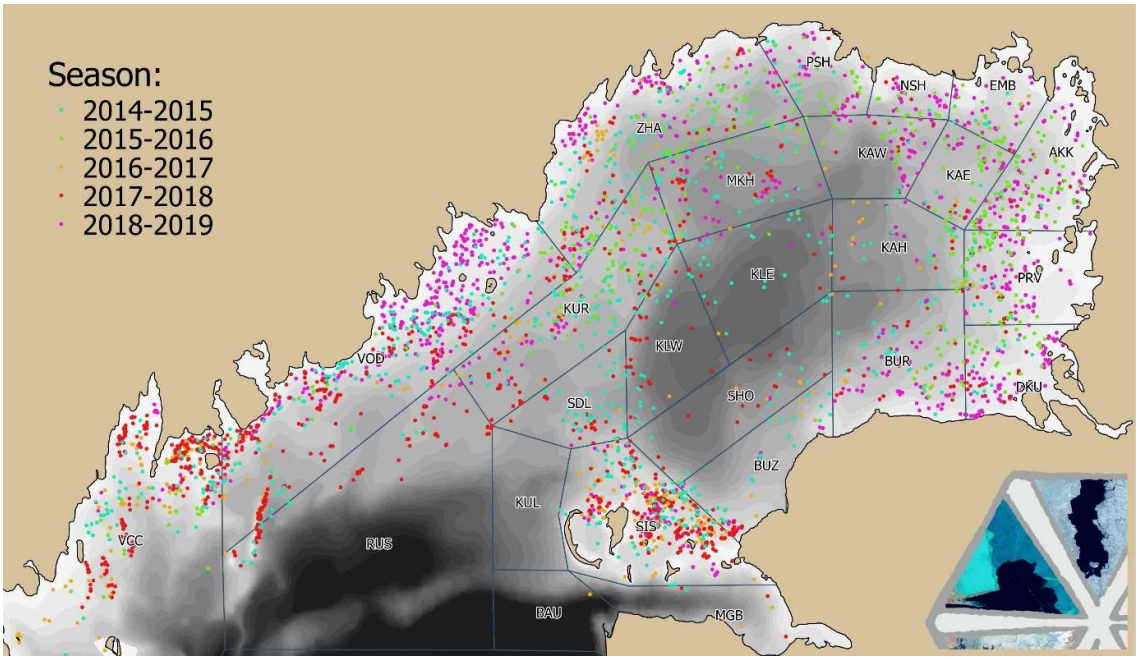

Figure 5: Stamukhi observations distribution across the Northern Caspian Sea as observed in the period from 2014 to 2019 (5 winters).

For the purpose of this study each stamukha record was supplemented with information on water depth, distance to coast, accumulated FDD until observation date in the area of location and averaged wind speed for 5 days prior to stamukha detection. Information on air

temperatures and wind regime was extracted from ERA5 ECMWF reanalysis.

The dataset of individual observations as presented in the figure above has its utilization limits to visualize dependencies from other environmental parameters as well as does not allow showing intensity of the phenomena in a comprehensive and analyzable manner. Concept for stamukhi visualization was taken from report about distribution of Antarctic icebergs by Romanov Y, 2011 and it is generally a regularly spaced grid containing average and cumulative values summarizing point observations for each cell. Based on several sensitivity experiments each grid cell's size was assigned 7.55 arcminutes along longitude and 5.39 arcminutes along latitude. This cell size corresponds to approximately 10x10 km that is more comprehensive for general public. Grid centroids were positioned geographically to have best compatibility with ERA5 reanalysis and forecast by ECMWF for easier correlation routines in future.

The major rationale behind using the size of grid was operational ice related risks analysis with this distance being sufficient for timely response to hazards within the cell for majority of vessels operating in the region. Figure 6 below illustrates the grid visualized as regularly spaced data with continuously tiled surface. Grid's coordinates are referencing the centroids of the tiles. Figure 6 illustrates the grid itself and all observations collected for the last 5 years. Seasonal cumulative area that is introduced in detail below shows intensity of phenomena distributed geographically while stamukhi count gives impression on frequency of occurrence.

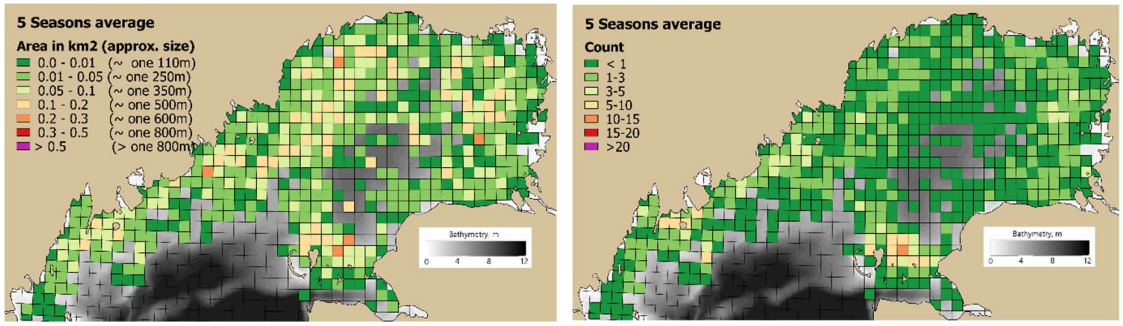

Figure 6: Seasonal cumulative area averaged over the period of observations (Left) and averaged number (Right) of all observed stamukhi sorted in 10x10 km grid for winters from 2014 to 2019.

Apart from parametric information like bathymetry, water level, accumulated FDD index and others needed for analysis each grid point contains the following information on stamukhi observed in the surrounding cell extracted from database of individual stamukhi observations that are considered in the scope of this study:

- Number of stamukhi that links the dataset to WMO based symbology for deformed ice features containing density of their distribution;
- Cumulative area of stamukhi surface is a normalizing parameter introduced to indicate intensity of stamukhi observations in each cell. Area of each stamukhi is calculated with rough approximation of a stamukha being circular shape with width of a stamukha assumed to be a diameter of the circle for the scope of this study. Summing areas of all stamukhi falling into cell over a season gives the index used for visual analysis of phenomena intensity at later stages;
- Average persistence is duration-based parameter resulting from averaged difference between erosion and detection date for all stamukhi falling into the cell.

Upon completion of data assimilation, we have received a tool for comparative analysis of stamukhi parameters to environmental conditions that have somehow led to their formation. Some of the insights on stamukhi phenomena dependency from key parameters recorded to describe sea ice behavior are presented in the section below.

MAJOR DEPENDENCIES

Complex structure of the resulting database allows extracting relationships between stamukhi parameters and oceanographic conditions in numerous combinations. Within the scope of this study we have tried to focus on ability to forecast stamukhi appearance by analyzing information on:

- Distribution and intensity of the phenomena across the whole region;
- Analysis of frequency and intensity dependencies from water depth and proximity to coast;
- Analysis of intensity dependencies from FDD and wind force.

These relationships are supposed to form a typical scenario of stamukhi formation and will allow estimating appearance, intensity and persistence based on weather forecast in future seasons to facilitate any operations that are sensitive to the phenomena. The same scenarios backed with statistical information can be used as the basis of design for pipelines and design of logistical concepts in support of developing offshore installations.

Distribution across Region

Distribution of observed stamukhi seasonal cumulative area in a grid averaged for all observations during the last 5 years (Figure 6) indicates areas with high frequency and intensity of the phenomena. Although this could be a good basis for choosing path of future pipeline and assessment of conditions for deployment of new offshore facilities it will not give correct picture for operational support during one season with its unique severity by accumulated degree-days and wind regime.

Figure 7 shows the last 5 seasons segregated into individual charts with spatial distribution of cumulative area and number of observed stamukhi. The last five seasons contained only normal and mild seasons based on accumulated FDD over the eastern part of the region if compared to the history of the last 20 years. So, it was not possible to assess stamukhi phenomena for severe winters.

As for differences in distribution of intensity it can be noted that there is little correlation between season severity rated by FDD. For example, number of cells with cumulative area exceeding 0.5 km^2 in 2014-2015 is highest, while the same number is higher for 2015-2016 (the mildest in the history) than for 2016-2017 which was significantly more severe.

Frequency of observations between normal winters also confirms that there are other mechanisms controlling spatial distribution of stamukhi phenomena. Season 2016-2017, for example stands out with low number of stamukhi over the whole region if compared to the other two normal winters. Similarly, for the two mild seasons while distribution of observations was mainly concentrated along the northern and eastern coasts in 2015-2016, it was similar to a normal winter's distribution in 2018-2019.

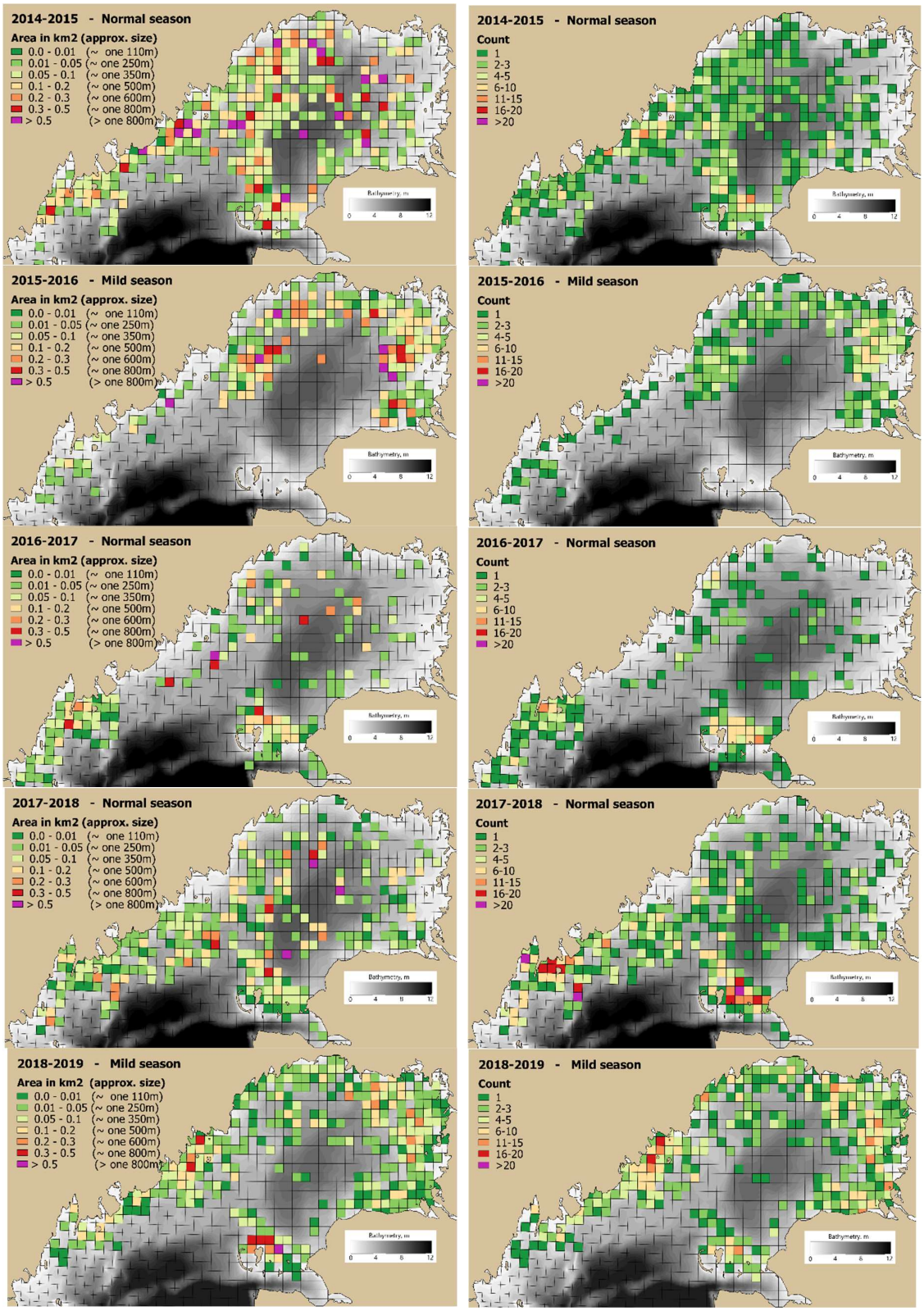

Figure 7: Cumulative area (Left) and number (Right) of stamukhi sorted in 10x10 km grid for each season from 2014 to 2019.

Stamukhi persistence

Persistence of stamukhi is defined as difference between detection date and the date when its disappearing was confirmed as melting date which in some cases extended weeks beyond the last day of ice cover presence. Figure 8 shows average persistence of stamukhi observed in each cell of the grid for each season from 2014 to 2019.

Similarly to spatial distribution of frequency and intensity of stamukhi observations discussed above, there is little correlation between persistence and geography of the region. Comparing ice season duration in the region with stamukhi persistence did not show any strong correlation either.

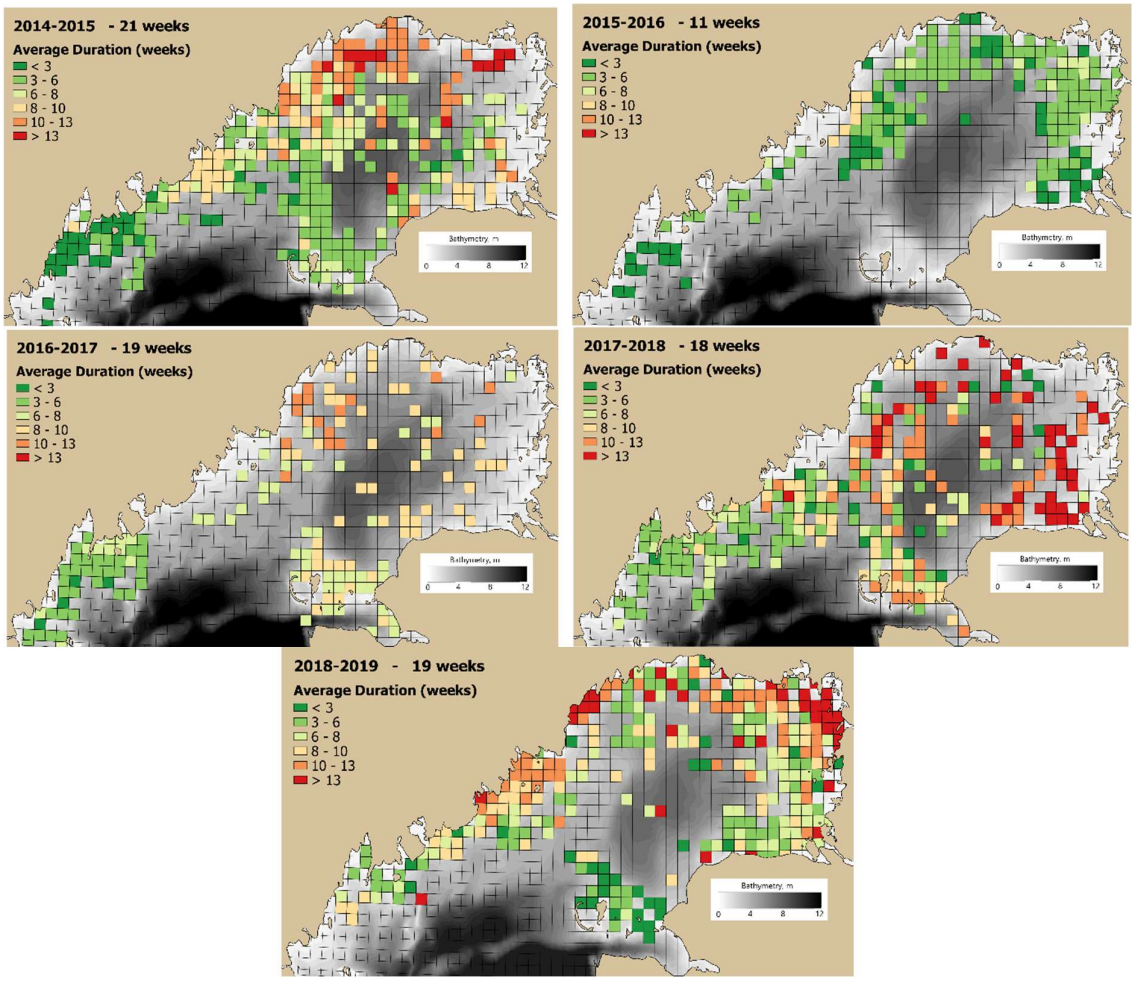

Figure 8: Average duration of stamukhi persistence sorted in 10x10 km grid for each season from 2014 to 2019.

Water depth and coast proximity

The dependency of stamukhi appearance in the certain areas was investigated by comparing stamukhi numbers and widths against water depth and proximity to coast for all stamukhi. Water depth at stamukha location was derived from 100x100 m bathymetry spatial grid and 0.5m vertical resolution by subtracting negative or adding positive annual average water level for each season. Wind induced water level variations were neglected in the scope of this study.

Distribution of stamukhi number by water depth (Figure 9) clearly shows that stamukhi were observed to form more often in water depths of 1 to 4.5 meters with higher intensity in the range from 1 to 2.5 m. Similar trend can be traced for stamukhi number distribution by distance to coast. The first 10 km along the coast coinciding with shallower waters contain less objects. Higher numbers of stamukhi are observed in 10-20 km and they gradually reduce to no observation 100 km away from coastline. Both distributions look similar which makes sense as generally increasing distance to coast leads to deeper waters in this region.

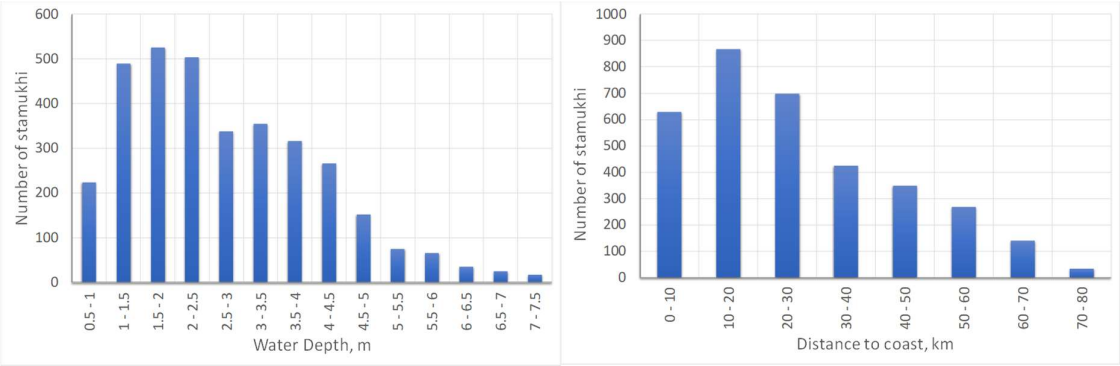

Figure 9: Number of stamukhi as observed in areas with varying water depth (Left) and distance to coast (Right).

Figure 10 shows the distribution of individual stamukhi widths as extracted from satellite imagery by water depth and proximity to coast line. Both figures indicate there is a trend of mean stamukhi width to increase with deeper water and further away from shores. Fluctuations of widths for water depth starting from 6 meters can be explained by smaller number of observations.

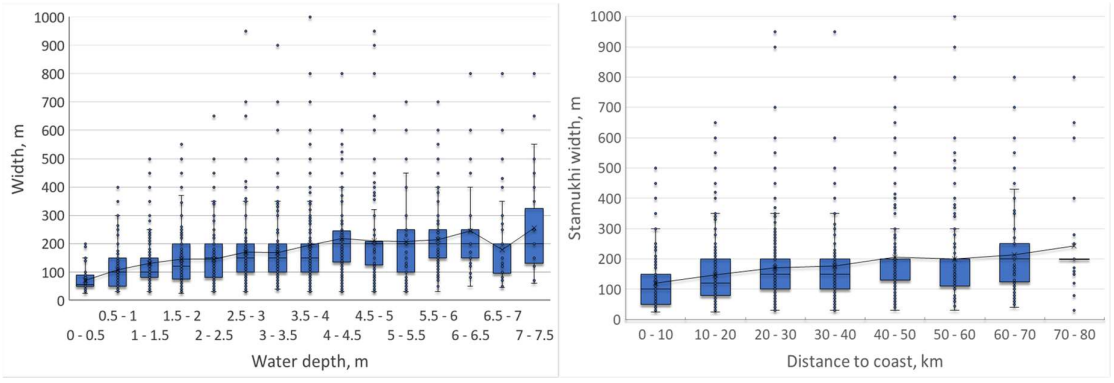

Figure 10: Stamukhi width distribution by water depth (left) and distance to coast (right). Curved line is average, Blue thick bar is 50% of observations, T Bar is 99.3% of observations, points are individual observations outside 99.3% of observed values.

The trends from Figure 9, Figure 10 make sense from general perspective as it correlates with our understanding of phenomena. One would expect that with proximity to shore water depths are small leading to high chance of stamukhi formation from almost every drift event when even small ridge keels will interact with seabed and trigger grounding processes. This effect stabilizes ice cover in the area along coast limiting further ice drift events and therefore growth of existing stamukhi. On the other hand, with deeper waters only large and rare ridge keels lead

to formation of stamukhi but should such stamukha form recurring drift events promote further growth of the feature (increasing width).

FDD

Assuming ice cover thickness is regulated with accumulated Freezing Degree-Days collected in the region and ice thickness has direct effect on size of stamukhi by limiting the height of the feature we attempted to find out if there is a certain relationship between the values. So FDD accumulated in the area of detection to the date of each stamukha detection was extracted from modified ERA5 reanalysis dataset by ECMWF (The European Centre for Medium-Range Weather Forecasts) for each observation. Figure 11 shows results of correlation attempt between stamukhi width (left) and numbers (right) versus FDD segregated into bins by sensitivity to derived thickness for all records in the database and regardless of winter severity or wind regime during the seasons.

Majority of observations did not show any clear relationship between stamukhi width and FDD. The only conclusion that can be made is that there is trend for stamukhi to increase their size if they were formed with ice that accumulated 400 to 450 degree-days based on limited number of observations. This probably has to do with stabilizing effect due to winter severity observed in the region when larger accumulated FDD leads to thicker ice and increasing area of stationary ice cover that does not lead to creation of deformed features.

This conclusion is partially confirmed with the second graph in Figure 11 illustrating number of stamukhi versus FDD and clear trend that majority of features formed with FDD values up to 200 degree-days when ice cover is still relatively thin and, thus, being still mobile.

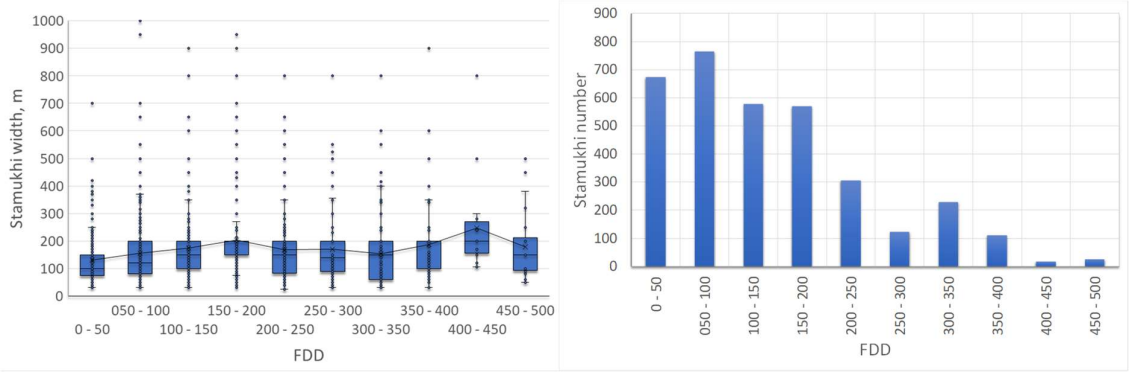

Figure 11: Stamukhi width (Left) and number (Right) distribution by FDD accumulated at the place of observation on the date of detection. Curved line is average, Blue thick bar is 50% of observations, T Bar is 99.3% of observations, points are individual observations outside 99.3% of observed values.

Wind

The other weather parameter that could help identifying stamukhi appearance is wind force that regulates possibility of drift and consequently forms a stamukha. Scalar wind speed from 5-day average wind vector over the area of detection and preceding detection date of each stamukha was extracted for each individual observation for this purpose. ERA5 reanalysis data by ECMWF was used to extract these values.

In order to reduce uncertainties with accuracy of detection data and timeliness of reanalysis data analysis was performed only for stamukhi observations that corresponded to events with

speeds above 10 knots (considered minimum threshold to trigger ice drift) with persistent direction. Wind direction persistence (95% of values falling in one 15-degree sector) was defined as no more than 1 knot difference between scalar and vector averaged wind speeds (equal values would represent persistent wind direction during the period).

Only one third of records (1089) answered wind direction persistence criteria and was used further down to extract dependencies (Figure 12). Distribution of stamukhi width sorted into bins of average 5-day wind speeds indicates continuously increasing likelihood of forming wider stamukhi with increasing wind speed although half of observations near average do not show any sensible trend.

Similarly, to other environmental factors discussed above, number of stamukhi observations have shown better relationship when compared with wind. The highest number of stamukhi formed under effect of average 5-day persistent in one direction wind with speeds ranging from 12 to 16 knots. Number of observations with stronger winds decreases significantly with each 2 knots step and there is little number of stamukhi that formed at speeds near drift threshold at 10-12 knots.

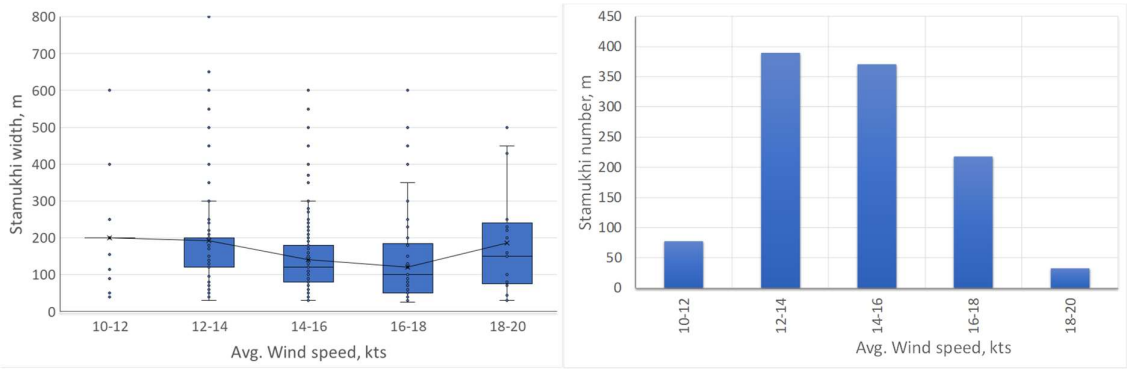

Figure 12: Stamukhi width (Left) and number (Right) distributed by 5-day average wind speed prior to detected date. Curved line is average, Blue thick bar is 50% of observations, T Bar is 99.3% of observations, points are individual observations outside 99.3% of observed values.

DISCUSSION

The stamukhi project itself led to development of efficient monitoring program and reliable database containing data that can be of use both for support of marine operations and future design activities. Results of the investigation based on this data both increased our understanding of mechanisms that control stamukhi formation across the Caspian region and revealed further steps for improving our knowledge of the phenomena.

Spatial distribution of frequency, intensity and persistence of stamukhi phenomena did not allow concluding there is any strong correlation to geographical location, FDD winter severity index or overall winter duration in the region. It can both be explained with little row of data available for analysis (only 5 years) or these indices simply don't have any correlation at all and should be investigated from other perspective like dependency from wind regime, for example.

The following clear relationships with environmental conditions leading to formation of stamukhi advance our forecasting abilities to support ongoing operations:

1. Stamukhi are likely to form more frequently in areas with water depths ranging from 1.0m to 2.5m. With less likelihood but still quite often stamukhi tend to form in the next segment of water depths ranging from 2.5m to 4.5m. Stamukhi forming in deeper waters than that will be a rare occasion, but their size will be generally bigger
2. Highest number of stamukhi is likely to be found in 10 to 20 km from shores with likelihood of their occurrence decreasing gradually further seawards.
3. Stamukhi tend to form when FDD accumulated over area of forecast is below 250 degree-days. However, the greatest ones form when FDD reaches 400-450 degree-days.
4. Wind persisting in one direction with five-day average speeds ranging from 12 to 18 knots are most favourable for stamukhi formation. The same value ranging from 10 to 12 knots can be considered threshold with minimum of previously observed stamukhi forming with this wind.

As for ability to forecast intensity of stamukhi formation there is still a lot of room for improvement. Apparently, the basic environmental indexes considered in this study have secondary effect on the process to define clear relationship with stamukhi sizes and need further investigation.

ACKNOWLEDGEMENTS

Authors would like to express their gratitude and appreciation to partnership of the Member States, the European Space Agency (ESA), the European Organization for the Exploitation of Meteorological Satellites (EUMETSAT), the European Centre for Medium-Range Weather Forecasts (ECMWF), EU Agencies and Mercator Océan that run Copernicus European Union's Earth Observation Program. Data distributed through this program forms the basis of this and many other studies performed by ICEMAN.KZ.

REFERENCES

Bukharitsin P., Sigitov A., Vernyayev S., Kadranov Y., Bukharitsin A., 2019. Marine Operations in Channels through Shallow Ice-Covered Waters. *Proceedings of the 25th International Conference on POAC*, POAC19

Hydrometeorology and Hydrochemistry of Seas. Volume VI. Caspian Sea. Edition I. Hydrometeorological conditions. 1992. Hydrometeoizdat: Saint-Petersburg, pp.125-359.

LLP ICEMAN.KZ, 2019. SatLog Summary (Updated 15 March 2019) Available at: ht tps://iceman.kz/data-access/satlog/ [Accessed 15 March 2019]

McKenna R., McGonigal D., Stuckey P., Crocker G., Marcellus B., Croasdale K., Verlaan P., Abuova A., 2011. Modelling of ice rubble accumulations in the North Caspian Sea. *Proceedings of the 21st International Conference on POAC*, POAC11-003.

Nilsen R, Verlaan P., 2011. The North Caspian Sea Ice Conditions and how Key Ice Data is Gathered. *Proceedings of the 21st International Conference on POAC, POAC11-003.*

Romanov, Y., Romanova, N., & Romanov, P. 2017. Geographical distribution and volume of Antarctic icebergs derived from ship observation data. *Annals of Glaciology*, 58(74), 28-40. doi:10.1017/aog.2017.2

Vernyayev, S., Debart, C., Kadranov, Ye., Sigitov, A., 2016. Operational ice charting in mid-latitudes using Near Real Time SAR imagery. *The Future of Geological Remote Sensing - GRSG*, London.